Diffusion from a Bottom Layer;

Diffusion with Moving Boundaries

STIG LJUNGGREN and OLE LAMM

The Royal Institute of Technology, Division of Physical Chemistry, Stockholm 70, Sweden

A new method of carrying out diffusion experiments is outlined, the initial condition being that the whole quantity of diffusing substance is concentrated in a thin layer at the bottom of the cell at zero time. Ideal equations are derived for uniform and non-uniform substances and a normalization procedure is described. The diffusion curves theoretically calculated for various binary mixtures of solutes are discussed and it is pointed out that in this type of diffusion the distortion of the curves due to non-uniformity is usually greater than that which occurs in ordinary diffusion. The apparatus and mode of operation are described in detail and a few experiments with uniform and non-uniform substances are related. In particular, mixtures of partially hydrolyzed dextran and sodium chloride were investigated.

I. INTRODUCTION

If pure solvent or a dilute solution of a single substance is levelled above a more concentrated solution of the same substance, so that the initial concentration difference equals $\Delta c°$ (Fig. 1), the resulting one-dimensional diffusion process will under ideal conditions be governed by the following equation [2,3]

$$\frac{\partial c}{\partial x} = \frac{\Delta c°}{2 \sqrt{\pi Dt}} e^{-x^2/4Dt},$$

where x denotes the position coordinate with reference to the original boundary surface, D the diffusion coefficient and t the diffusion time. If a linear relation is assumed between the concentration and the refractive index of the solution (which holds fairly accurately in most cases), the concentration gradient can be measured, using, *e. g.*, the scale method.

For non-uniform diffusion, *i. e.* if there are two or more components with different diffusion coefficients present, this equation is not valid. This fact may be utilized as an indication of non-uniformity. Thus it was shown by Lamm [1] that in normal coordinates the curve of a non-uniform diffusion

Fig. 1. Principle of "ordinary" diffusion.   *Fig. 2.* Principle of bottom layer diffusion.

process will always have a positive excess at the axis of symmetry as com-
pared to the curve of uniform diffusion. Theoretically the shape of an experi-
mentally obtained curve would even permit the distribution function of dif-
fusion coefficients to be calculated using numerical methods, although the
experimental accuracy is as a rule too low for this to be practical.

It was pointed out by Lamm [2] that ordinary diffusion is by no means the
ideal process for indicating non-uniformity. The uniform diffusion curves of
the single components, which combine to give the resulting compound curve,
will all have a mutual axis of symmetry at the position of the original boun-
dary. This results in rather a close amalgamation of the curves.

It seems, therefore, that if the diffusion could be arranged with a different
initial condition so that the resulting uniform diffusion curve was non-sym-
metrical, non-uniformity would be more clearly displayed. Such a possibility
is offered by diffusion from a bottom layer, where the diffusion starts out
from a very thin layer of relatively concentrated solution at the bottom of the
cell, levelled below pure solvent (Fig. 2). If the bottom layer is infinitely thin
and if the influence of the concentration on the diffusion coefficient is neglec-
ted, the equation of uniform diffusion from bottom layer can be written [3]

$$\frac{\partial c}{\partial x} = - \frac{Ax}{2 \sqrt{\pi} \, D^{3/2} t^{3/2}} \, e^{-x^2/4Dt}$$

where x is the height above the bottom of the cell. This function is the first
derivative with respect to x of the above function for "ordinary" diffusion
and it is non-symmetrical, as is seen from Fig. 3. Further it is easily seen that
the abscissa of the maximum point depends on D and t. Some elementary
properties of the function will be given for convenience in the theoretical
section below. In cases, however, where non-uniformity is not very pro-
nounced, a direct comparison with the ideal curve suggests itself. In order
that this be possible, the curve must be plotted in normal coordinates inde-
pendent of time and other general experimental conditions. The normaliza-
tion procedure, analogous to that applied in connection with "ordinary"
diffusion, rests on the calculation of moments and it will be shown that the
first moment can advantageously be used for the normalization.

In this connection it may be worth mentioning that the first "absolute"
moment can also be used for the normalization of "ordinary" diffusion curves
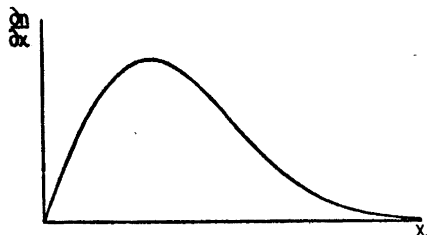in place of the second moment ordinarily used.

Fig. 3. Ideal curve for uniform bottom layer diffusion, according to eqn. (4).

II. THEORETICAL

a) Elementary properties of the uniform curve

If A moles per cm² are concentrated to $x = 0$ at the time $t = 0$ (Fig. 2), the following equation will now hold for the concentration (compare above)

$$\bar{c} = \frac{A}{\sqrt{\pi Dt}} \, e^{-x^2/4Dt} \tag{1}$$

The bar above c denotes that we are dealing with a uniform case. This mode of notation will be generally adopted in the subsequent discussion. Derivation with respect to x yields

$$\frac{\partial \bar{c}}{\partial x} = - \frac{Ax}{2 \sqrt{\pi} \, D^{3/2} t^{3/2}} \, e^{-x^2/4Dt} \tag{2}$$

If a linear relation is assumed between refractive index and concentration [4],

$$n = n^\circ + Rc \tag{3}$$

we obtain for the refractive index gradient

$$-X = \frac{\partial \bar{n}}{\partial x} = - \frac{RAx}{2 \sqrt{\pi} \, D^{3/2} t^{3/2}} \, e^{-x^2/4Dt} \tag{4}$$

For the abscissa of the maximum point we get

$$\bar{x}_m^2 = 2Dt \tag{5}$$

and for the abscissa of the point of inflexion

$$\bar{x}_i^2 = 6Dt \tag{6}$$

Thus

$$\bar{x}_i/\bar{x}_m = \sqrt{3} \tag{7}$$

The area of the curve is

$$\Phi = -\int_0^\infty \frac{\partial \bar{n}}{\partial x} \, dx = \int_0^\infty \bar{X} dx = \frac{RA}{\sqrt{\pi Dt}} \tag{8}$$

and the maximum ordinate is obtained if x_m is inserted into (4):

$$\bar{X}_m = \frac{RA}{\sqrt{2\pi e Dt}} \tag{9}$$

Hence

$$\frac{\Phi^2}{\overline{X}_m^2} = 2eDt \tag{10}$$

The ordinate of the point of inflexion is

$$\overline{X}_i = \frac{RA\sqrt{6}}{2e\sqrt{\pi eDt}} \tag{11}$$

Thus

$$\frac{\overline{X}_i}{\overline{X}_m} = \frac{\sqrt{3}}{e} \tag{12}$$

The slope of the curve at the point of inflexion is

$$\left(\frac{\partial \overline{X}}{\partial x}\right)_i = \frac{-RA}{\sqrt{\pi e^3 D^3 t^3}} \tag{13}$$

But the slope at $x = 0$ is

$$\left(\frac{\partial \overline{X}}{\partial x}\right)_{x=0} = \frac{RA}{2\sqrt{\pi D^3 t^3}} \tag{14}$$

Hence

$$\left(\frac{\partial \overline{X}}{\partial x}\right)_{x=0} = -\frac{e^{3/2}}{2}\left(\frac{\partial \overline{X}}{\partial x}\right)_i$$

The slope of a line combining the maximum point with the origin is

$$\frac{\overline{X}_m}{x_m} = \frac{RA}{2\sqrt{\pi eD^3 t^3}} \tag{15}$$

Thus

$$\frac{\overline{X}_m}{x_m} = \frac{1}{\sqrt{e}}\left(\frac{\partial \overline{X}}{\partial x}\right)_{x=0} = -\frac{e}{2}\left(\frac{\partial \overline{X}}{\partial x}\right)_i \qquad \text{(Fig. 5)} \tag{16}$$

A combination of some of the foregoing expressions yields

$$\frac{x_i \overline{X}_m}{\left(\dfrac{\partial \overline{X}}{\partial x}\right)_i} = Dt\, e\sqrt{3} \tag{17}$$

In case it should be difficult to find the exact position of the origin, the width of the curve, δ, at the ordinate of the inflexion point (Fig. 4) may be used. By the use of the tables of Jahnke and Emde it is found that

$$\delta \approx 1.852\,\sqrt{Dt} \tag{18}$$

Hence

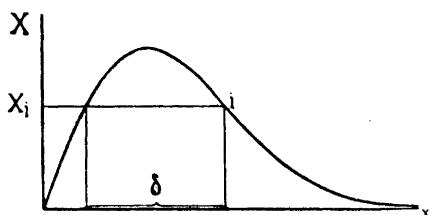$$Dt \approx \frac{\delta^2}{3.43} \tag{19}$$
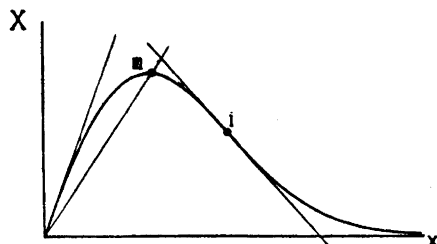
Fig. 4. "Width" of ideal curve.

Fig. 5. Elementary properties of bottom layer diffusion curves.

For the calculation of the diffusion coefficient, relations (5), (6), (10), (17) and (19) may be used.

b) Relations for non-uniform curves

We will now assume that there are several components present, each of which diffuses independently of the others, $i.\,e.$ the Arrhenius-Thovert effect is neglected. Then

$$-X = \frac{\partial n}{\partial x} = \sum_{i=1}^{q} \frac{\partial n_i}{\partial x} = -\sum_{i=1}^{q} \frac{R_i A_i x}{2\sqrt{\pi}\, D_i^{3/2} t^{3/2}}\, e^{-x^2/4D_i t} \tag{20}$$

owing to the additive property of the refractive index contributions. If the number of substances were increased infinitely, the sum of eqn. (20) would go over into an integral. For the sake of generality we define a distribution function, $f\,(D)$, such that

$$d(RA) = f(D)\, dD$$

The expression equivalent to eqn. (20) will then be

$$-X = \frac{\partial n}{\partial x} = -\frac{1}{2\sqrt{\pi}} \int_0^\infty \frac{x}{D^{3/2} t^{3/2}}\, e^{-x^2/4Dt}\, f(D)\, dD \tag{21}$$

A discontinuous distribution case cannot be described exactly by eqn. (21) but it can be approximated with any desired degree of accuracy. The calculation of the maximum and inflexion point coordinates of a non-uniform curve does not give any simple explicit result. From a practical point of view, however, it is obvious that at least in cases of pronounced non-uniformity there will be a deviation from the conditions of eqn. (16).

c) Moment expressions

The r:th moment of the refractive index gradient curve is defined in the following way

$$m_r = \int_0^\infty x^r X dx = -\int_0^\infty x^r \frac{\partial n}{\partial x}\, dx \tag{22}$$

Obviously the moment of order zero is identical with the area of the curve, previously denoted by Φ:

$$m_0 = \Phi$$

Substituting for X the expression of eqn. (21) we obtain

$$m_r = \frac{1}{2\sqrt{\pi}} \int_0^\infty x^r dx \int_0^\infty \frac{x}{D^{3/2}t^{3/2}} e^{-x^2/4Dt} f(D) \, dD \tag{23}$$

By the substitution

$$\zeta = x / 2 \sqrt{Dt}$$

(23) is transformed into

$$m_r = \frac{2^{r+1} t^{(r-1)/2}}{\sqrt{\pi}} \int_0^\infty f(D) D^{(r-1)/2} \, dD \int_0^\infty \zeta^{r+1} e^{-\zeta^2} \, d\zeta$$

We will abbreviate

$$\mu_r = \int_0^\infty f(D) D^{(r-1)/2} \, dD \tag{24}$$

Hence

$$m_r = \frac{2^r t^{(r-1)/2}}{\sqrt{\pi}} \Gamma\left(\frac{r+2}{2}\right) \mu_r = \alpha \cdot \mu_r \tag{25}$$

since

$$\int_0^\infty \zeta^{r+1} e^{-\zeta^2} \, d\zeta = \frac{1}{2} \Gamma\left(\frac{r+2}{2}\right)$$

provided that $r + 2 > 0$, or $r > -2$.

For convenience the factor, $\alpha = \dfrac{1}{\sqrt{\pi}} \, 2^r t^{(r-1)/2} \, \Gamma\left(\dfrac{r+2}{2}\right)$, is listed in Table 1 for some values of r.

Table 1.

r	α
0	$1/\sqrt{\pi t}$
1	1
2	$4\sqrt{t}/\sqrt{\pi}$
3	$6t$
4	$32t^{3/2}/\sqrt{\pi}$

The reduced moments of the distribution function are defined as follows:

$$\mathscr{D}_{rm}^{r/2} = \frac{\mu_r}{\mu_0} ; \qquad \mathscr{D}_{rm} = \left(\frac{\mu_r}{\mu_0}\right)^{2/r} \tag{26}$$

In the uniform case, (24) reduces to

$$\bar{\mu}_r = RAD^{(r-1)/2} \tag{27}$$

Hence

$$\bar{\mathscr{D}}_{rm} = D \tag{28}$$

Relation (28) provides a method for obtaining the diffusion coefficient from an experimental curve. For the calculation of moments the use of Simpson's formula is recommended.

If the error in a moment computed from an experimental curve is $\delta\ m_r$, then the error in the reduced moment calculated according to eqn. (26) will be

$$\left| \frac{\delta\ \mathscr{D}_{rm}}{\mathscr{D}_{rm}} \right| = \left| \delta \ln \mathscr{D}_{rm} \right| = \frac{2}{r} \cdot \left| \delta \ln \frac{\mu_r}{\mu_0} \right|$$

or

$$\frac{\delta\ \mathscr{D}_{rm}}{\mathscr{D}_{rm}} = \frac{2}{r} \left| \frac{\delta\ m_r}{m_r} \right| + \frac{2}{r} \left| \frac{\delta\ m_0}{m_0} \right| \tag{29}$$

Since the error in a moment calculated from an experimental curve increases greatly with increasing r, it should be possible to find an optimum value of r, depending on the experimental degree of accuracy, which gives $|\delta\ \mathscr{D}_{rm} / \mathscr{D}_{rm}|$ a minimum value. For practical purposes it seems reasonable to use the first moment.

d. Normalization

By the linear transformations

$$\varXi = - \frac{\sqrt{\mathscr{D}_{rm}t}}{m_0} \frac{\partial\ n}{\partial\ x} \tag{30}$$

$$\xi = x/2 \sqrt{\mathscr{D}_{rm}t}$$

the equation of uniform diffusion is transformed into

$$\varXi = \xi \cdot e^{-\xi^2} \tag{31}$$

since, in the uniform case,

$$\bar{m}_0 = RA/\sqrt{\pi Dt}$$

$$\bar{\mathscr{D}}_{rm} = D$$

The normalized curve is independent of time. In the discussion below it will be assumed that $\mathscr{D}_{1m}$ has been used for the normalization. In non-uniform cases, the normalized curve will deviate from the curve of eqn. (31). The applied mode of normalization implies that the first and zero moments will always be identical with those of the ideal curve, *i. e.* the area and the ξ-coordinate of the point of gravity of all normalized curves will have fixed values.

e. Recognition of non-uniformity

From the foregoing we recall that

$$\mu_r = \int_0^\infty f(D) \ D^{(r-1)/2} \ dD \tag{24}$$

and

$$\bar{\mu}_r = RAD^{(r-1)/2} \tag{27}$$

Hence

$$\bar{\mu}_p = \bar{\mu}_r^{-\alpha} \bar{\mu}_s^{-\beta} \tag{32}$$

if

$$p = \alpha r + \beta s; \quad \alpha + \beta = 1$$

By a simple application of the Hölder inequality it can be shown that

$$\mu_p < \mu_r^\alpha \mu_s^\beta \tag{33}$$

if $p = \alpha r + \beta s$, $\alpha, \beta > 0$, $\alpha + \beta = 1$
From (32) and (33) it follows that for $\mu_r = \bar{\mu}_r$ and $\mu_s = \bar{\mu}_s$

$$\mu_p < \bar{\mu}_p \tag{34}$$

if

$$r < p < s$$

In a similar manner we find that

$$\mu_p > \bar{\mu}_p \tag{35}$$

if

$$p < r \ \text{or} \ p > s, \ r < s$$

These relations can be applied to show that the slope at $\xi = 0$ of a non-uniform curve in normal coordinates is always greater than that of the uniform curve.

Other elementary methods for recognizing non-uniformity rest on a comparison of the values of the diffusion coefficient obtained by different methods (5), (6), (10), (17) and (19). As already mentioned, there will also be a deviation from eqn. (16) in non-uniform cases. Depending on the nature and degree of non-uniformity present, the eye will be more or less sensitive to the deviation from the shape of the ideal curve.

f. Non-uniformity in two-component cases

The simplest non-uniform cases are those where there are only two diffusing components present, denoted by the respective indices 1 and 2. If the following two parameters are introduced

$$\beta = R_1 A_1 \ / \ R_2 A_2 \tag{36}$$

$$\gamma = V\overline{D_1 / D_2}$$

the compound curve in its normalized form can be written

$$\varXi = \varXi_1 + \varXi_2 \tag{37}$$

where

$$\varXi_1 = \frac{\beta(\beta + 1)}{(\beta + \gamma)^2}\, e^{-\xi_1^2}\, \xi_1; \quad \xi_1 = \frac{\beta + 1}{\beta + \gamma}\, \xi \tag{38}$$

$$\varXi_2 = \frac{\gamma^2(\beta + 1)}{(\beta + \gamma)^2}\, e^{-\xi_2^2}\, \xi_2, \quad \xi_2 = \frac{\gamma(\beta + 1)}{\beta + \gamma}\, \xi \tag{39}$$

Here $\varXi_1$ and $\varXi_2$ are the respective contributions from the two components. In the case of "ordinary" diffusion, the corresponding equations are

$$\varXi_1 = \frac{2}{\sqrt{\pi}}\, \frac{\beta(\beta\gamma + 1)}{\gamma(\beta + 1)^2}\, e^{-\xi_1^2}; \quad \xi_1 = \frac{\beta\gamma + 1}{\gamma(\beta + 1)}\, \xi \tag{40}$$

$$\varXi_2 = \frac{2}{\sqrt{\pi}}\, \frac{\beta\gamma + 1}{(\beta + 1)^2}\, e^{-\xi_2^2}; \quad \xi_2 = \frac{\beta\gamma + 1}{\beta + 1}\, \xi \tag{41}$$

For a comparison between the two methods, the following six cases are reproduced in normal coordinates along with the uniform curve, denoted by index zero

Curve No.	β	γ
1	5	2
2	1	2
3	10	4
4	1	4
5	100	4
6	1/100	4

in Figs 6, 7 and 8 for diffusion from a bottom layer and in Figs 9, 10 and 11 for "ordinary" diffusion. Especially important from the point of view of judging the relative merits of the two methods are cases 5 and 6, where one of the components is present only in minute amounts, *i. e.* may be regarded as a
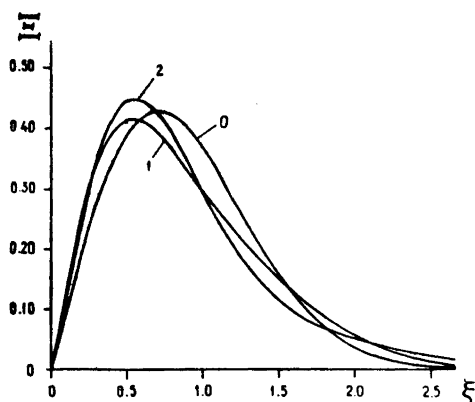

Fig. 6. Normalized curves for two-component cases. Bottom layer diffusion. 0, Ideal curve; 1, $\beta = 5$, $\gamma = 2$; 2, $\beta = 1$, $\gamma = 2$.
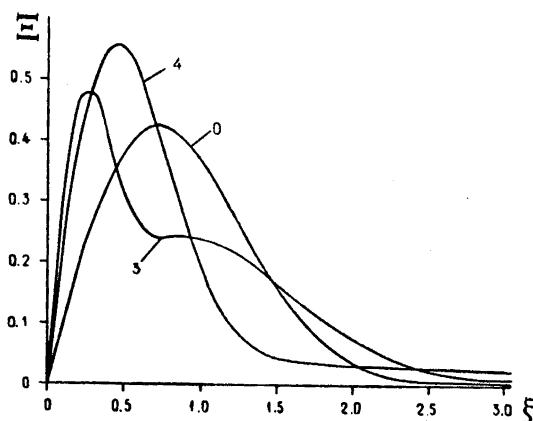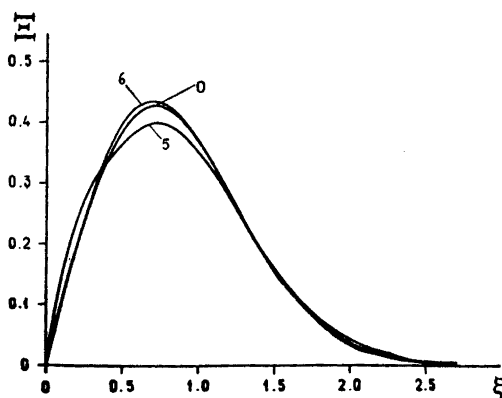
Fig. 7. Normalized curves for two-component cases. Bottom layer diffusion. 0, Ideal curve; 3, $\beta = 10$, $\gamma = 4$; 4, $\beta = 1$, $\gamma = 4$.

contamination. As appears from the figures, the assymmetrical character of the curves for bottom layer diffusion will generally cause a considerable deviation from the ideal curve to occur over a greater range of abscissa values. Further it is seen that the bottom layer method is particularly favourable when the "contamination" has a lower diffusion coefficient than the main component (Fig. 8). From the equations above, it is found that if

$$\eta = \frac{(\varXi \text{ contaminant})_{\text{max}}}{(\varXi \text{ main.comp.})_{\text{max}}}; \qquad \gamma > 1 \tag{42}$$

then

$$\text{for } \beta > 1; \; \eta' = \frac{(\varXi_2)_{\text{max}}}{(\varXi_1)_{\text{max}}} = \frac{\gamma^2}{\beta} \tag{43}$$

and

$$\text{for } \beta < 1; \; \eta'' = \frac{(\varXi_1)_{\text{max}}}{(\varXi_2)_{\text{max}}} = \frac{\beta}{\gamma^2} \tag{44}$$

Fig. 8. Normalized curves for two-component cases. Bottom layer diffusion. 0, Ideal curve; 5, $\beta = 100$, $\gamma = 4$; 6, $\beta = 1/100$, $\gamma = 4$.
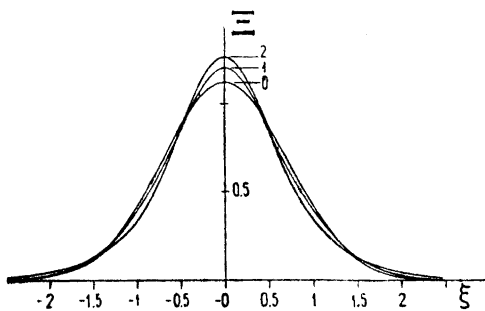
Fig. 9. Normalized curves for two-component cases. "Ordinary" diffusion. 0, Ideal curve; 1, $\beta = 5$, $\gamma = 2$; 2, $\beta = 1$, $\gamma = 2$.
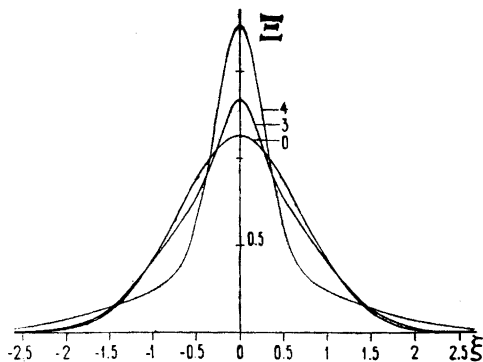

Fig. 10. Normalized curves for two-component cases. "Ordinary" diffusion. 0, Ideal curve; 3, $\beta = 10$, $\gamma = 4$; 4, $\beta = 1$, $\gamma = 4$.

Thus

$$\eta' / \eta'' = \gamma^4 \tag{45}$$

i. e. the former case is greatly favoured. For "ordinary" diffusion we have

$$\eta' = \frac{\gamma}{\beta}, \; \eta'' = \frac{\beta}{\gamma} \tag{46}$$

Hence

$$\eta' / \eta'' = \gamma^2 \tag{47}$$

Further it can be shown that the excess,

$$\Delta = \varXi_{\max} - \overline{\varXi}_{\max} = \frac{\beta}{\gamma} \frac{(\gamma - 1)^2}{(\beta + 1)^2} \tag{48}$$

Thus

$$\Delta(\beta) = \Delta(1 / \beta) \tag{49}$$

i. e. the excess is independent of whether the "contamination" has a greater or smaller diffusion coefficient than the main component, although in the former case the excess will occur over a greater range of abscissa values.
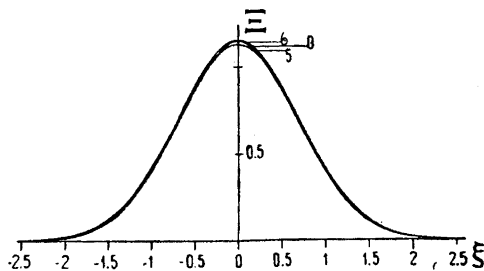
Fig. 11. Normalized curves for two-component cases. -'Ordinary" diffusion. 0, Ideal curve; 5, $\beta - 100$, $\gamma - 4$; 6, $\beta - 1/100$, $\gamma - 4$.

From the above arguments it is concluded that in cases of very low β and large γ, the "ordinary" diffusion method would be favoured in comparison with diffusion from bottom layer from the point of view of recognizing non-uniformity. This is evidently true, but rather extreme conditions are probably required to outweigh the advantages of the bottom layer method. As is seen in case 6, the two methods are practically equal even for $\beta = \dfrac{1}{100}$, $\gamma = 4$. Thus it is concluded that, for most practical purposes, diffusion from a bottom layer is a more sensitive means of detecting non-uniformity.

Note: In eqns. (38), (39) and (40), (41) the "ordinary" diffusion curves are assumed to have been normalized using the first absolute moment. Some words on this method may therefore be apposite.

If the moments are defined in the usual way

$$m_r = \int\limits_{-\infty}^{+\infty} x^r X \mathrm{d}x \tag{50}$$

it is obvious that all moments of odd order will disappear, due to the symmetrical shape of the curves. This fact may even be utilized to find the position of the axis of symmetry. For this reason, the second moment has usually been employed for the normalization.

If we instead introduce the "absolute" moments

$$M_r = \int\limits_{-\infty}^{+\infty} |x|^r X \mathrm{d}x \tag{51}$$

which can be readily calculated from an experimental curve, it can be shown that

$$M_r = \alpha' \mu_{r+1} \tag{52}$$

where u_{r+1} is defined according to eqn. (24) and

$$\alpha' = \frac{1}{\sqrt{\pi}}\ 2^r t^{r/2}\ \Gamma\left(\frac{r+1}{2}\right) \tag{53}$$

The reduced moments are then defined by

$$\mathscr{D}_{rM} = \left(\frac{\mu_{r+1}}{\mu_1}\right)^{2/r} \tag{54}$$

and normalization is effected by the transformations

$$\varXi = \frac{4\ \sqrt{\mathscr{D}_{rM}t}}{M_0}\ X \tag{55}$$

$$\xi = x\ /\ 2\ \sqrt{\mathscr{D}_{rM}t}$$

III. EQUIPMENT AND OPERATION

a. *The thermostat*. The thermostat, shown in Fig. 12, had the outside dimensions, $31 \times 36 \times 33$ cm. It was insulated by 3 cm thick insulating cork, C, painted black, and protected from radiation losses by aluminium foil. The distilled water serving as thermostat liquid was stirred by a propeller stirrer driven by an almost vibrationless electric motor, B. The temperature control system was the usual one, including a contact thermometer, D, a relay and a dip-heater, E. A precision thermometer F enabled temperature fluctuations of 0.002 °C to be measured. The cell was placed between two brass blocks in position A. Slits in the brass blocks and a tube passing through the thermostat gave free passage to the light beam. The thermostat was mounted on a rider of a very stable (lathe type) optical bench, which in turn rested on a solid foundation.

The temperature fluctuations of the thermostat liquid never exceeded ± 0.002° C during the experiments.
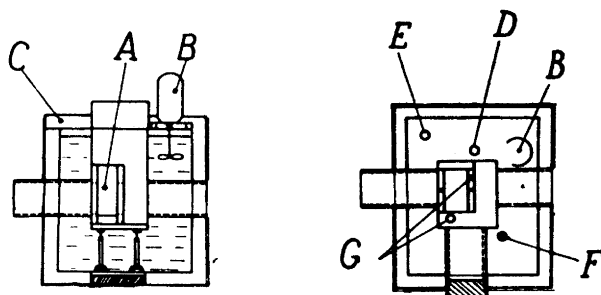
Fig. 12. Thermostat. A, cell position; B, electric stirrer motor; C, cork insolation; D, position for contact thermometer; E, Immersion heater; F, position for precision thermometer; G, position for thermometers for air and brass-block temperatures.

b. *The diffusion cell*. In the construction of the cell and the levelling arrangement the greatest possible simplicity was aimed at, simultaneously as the risk of convection and leakage had to be duly considered.

The cell was composed of plane parallel glass plates as shown in Fig. 13, the inner dimensions being: height 7.9 cm, bottom area 3×3 cm². At the center of the bottom plate there was a small hole filled with mercury into which the cannula of a tuberculine syringe dipped. The mercury served the double purpose of preventing the syringe leaking and of preventing cascade formation on injection of the bottom layer. The plexi-glas cover of the cell was provided with two holes, one for the cannula and one for the introduction of the solvent. To enable a slow and vibrationless operation of the syringe, a simple device was constructed, which included a micrometer screw acting directly upon the piston, Fig. 14. One turn of the screw corresponded to an injected volume of 0.008 ml.
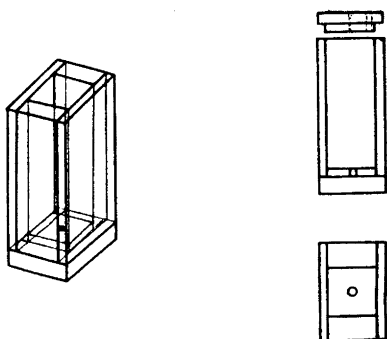
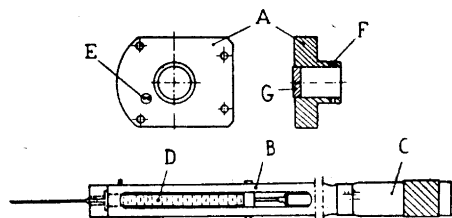Fig. 13. Diffusion cell with plexi-glas cover.

Fig. 14. Injection device. A, holder; B, syringe holder; C, micrometer screw, D, syringe; E, hole for the introduction of solvent; F, socket for B; G, rubber washer.

The cell fitted precisely into the space between two brass blocks in the thermostat, A, Fig. 12, and the holder of the injection device was screwed fast to the brass blocks. Fig. 15 shows the final arrangement with the cell in position in the thermostat.

c. *The optical arrangement.* The optical arrangement, schematically shown in Fig. 16, was based on the Svensson short focus modification of the scale method [5]. As suggested by Lamm [6], the diffusion cell was placed on the "plate" side of the lens system. The Svensson modification claims the advantage of reducing the length of optical bench required, without neglecting the
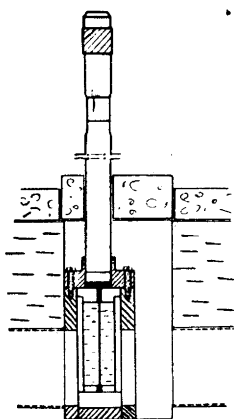
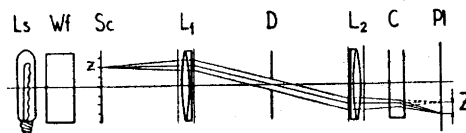Fig. 15. Cell in position in the thermostat.

Fig. 16. Schematic outline of optical arrangement. Ls, light source; Wf, water filter; Sc, original scale; L_1 and L_2, astronomical objectives; D, diaphragm; C, diffusion cell; Pl, photographic plate; z, scale line number; Z, scale line displacement.
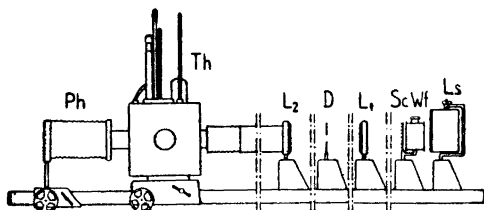
Fig. 17. Experimental set up. Ph, plate holder; Th, thermostat; L_1 and L_2, objectives; D, diaphragm; Sc, glass scale; Wf, water filter; Ls, light source.

demand for parallel or nearly parallel light through the cell. The condition is, however, that the focal distances of the lenses chosen should be sufficiently small. With focal distances of around 120 cm as used in our experiments, the necessity of using the Svensson method is debatable; it also limits the non-distorted part of the image. The diaphragm diameter used was 1.4 cm, which corresponds to an aperture of approx. 1 : 86. A precision glass scale with a scale constant of 0.399 mm was used. Fig. 17 shows the actual arrangement. During the experiments, however, the injection device was insulated by a tube of aluminium foil, lined with cotton.

The adjustment of the optical system was carried out by means of a telescope provided with cross-hairs adjusted for infinity. An illuminated scale was observed through the telescope and one of the lenses of the optical system and the position of the scale adjusted until no parallax between the cross-hairs and the scale remained. The scale was then assumed to be in the focal plane of the lens.

d. *Mode of operation.* The carefully cleaned and dried cell was then inserted in the thermostat. The syringe was filled with the solution to be injected and the top of the piston was greased to prevent vibrations while the micrometer screw was being turned. The syringe was placed in its holder, and the cannula carefully wiped. The injection device was then placed in position in the thermostat and screwed fast. Through the hole in the glass and plexi-glas covers, 50 ml of freshly boiled distilled water of a temperature slightly exceeding that of the thermostat was introduced by means of a cannula, connected with a separatory funnel by a polythene tube. After the introduction of the water the hole was plugged with cotton wool and the cork cover of the thermostat was put on. The thermostat was left for temperature equilibration, the mercury preventing the syringe from leaking. The bottom layer was then injected by slowly turning the micrometer screw at a uniform rate. The process could be followed on the ground glass plate. The time required for injection was 3—4 min, which, of course, introduces a small time-dependent non-uniformity since the diffusion constant always appears in eqn. (4) in connection with the time. The height of the injected layer was approx. 0.4 mm. Obviously it is desirable that the height of the bottom layer should be as small as possible, if the simple eqn. (4) is to be valid. This, however, requires that the bottom of the cell should be nearly perfectly horizontal.

The scale pictures were recorded on 6 × 9 process plates with one exposure per hour during the first 6 h of the experiment. The best exposures were obtain-

ed several hours (3 or 4 h with KCl) after the experiment had been started. During the first few hours, while the concentration gradient was still very high, the effective part of the scale was considerably blurred, owing to the defocussing effect of the gradient. This is, however, not serious for the accuracy of the measurement [1].

IV. EXPERIMENTS

A. Experiments with uniform substances

Experiment 1. In order to test the method, experiments with uniform substances were first conducted. 0.4 ml of 0.5 N KCl (analytical reagent) was injected. The thermostat temperature was 24.78 °C. Exposures were taken before the beginning of the levelling and after 2, 3, 4, 5 and 6 h. The scale photographs were comparated in the usual manner and the corresponding curves drawn, Fig. 18. The parts of the scales corresponding to low values of x were rather diffuse, due to the cutting-off effect of the cell bottom. For this reason it was difficult to find the exact Z-value corresponding to $x = 0$. By a consideration of various elementary properties of shape (rel. (20)), however, the position of the origin was estimated.

The curve taken after 4 h was normalized in the way described above and the ideal curve was drawn for comparison, Fig. 19. As appears from the diagram, the experimental difficulties have not yet been overcome. At present, however, it is difficult to judge whether the deviation is due to the systematic short-comings of the method of levelling or to other experimental circumstances.
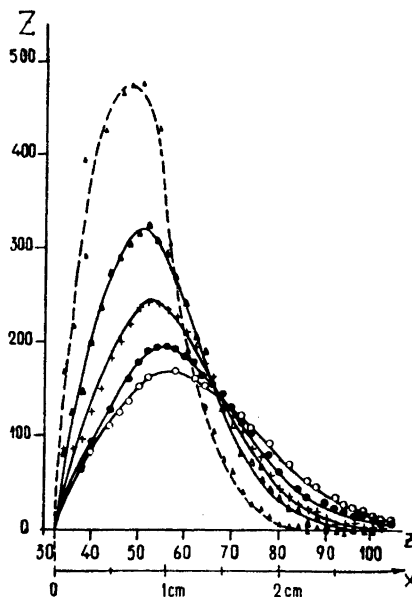

Fig. 18. Experimental (z, Z)-curves for the diffusion of potassium chloride in water at 24.78°C. Expt. 1.
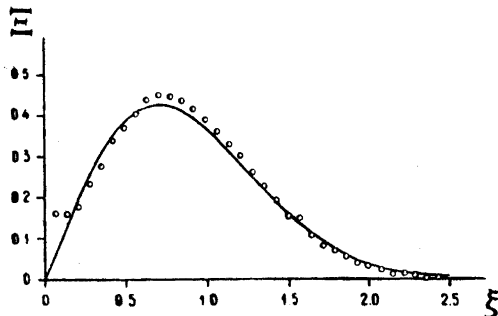
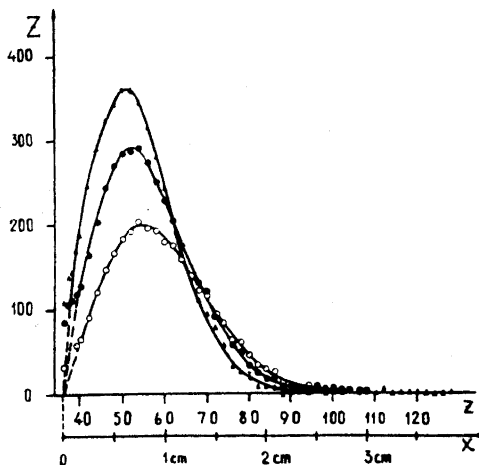Fig. 19. Points of normalized 4-h curve of expt. 1 together with normal ideal curve.

Fig. 20. Experimental curves from expt. 2. NaCl in water at 24.77°C. Filled triangles, 3-h curve; filled circles, 4-h curve; empty circles, 5-h curve. The deviation from the ideal shape of the curve for low values of x is probably due to minute amounts of high-molecular impurities.

Experiment 2. 0.4 ml of a 3 % NaCl solution was injected. Curves analogous to those for KCl were obtained.

In expt. 2 as in expt. 1, it was noted that the deviation from the ideal shape of curve for low x is not altogether irregular but exhibits a positive tendency. This is probably due to the presence of quite minute amounts of high-molecular impurities, which will cause, even at very low concentrations, an appreciable deviation from the ideal curve (compare Fig. 8).

The diffusion coefficient was calculated according to the maximum point, the inflexion point and the "width" methods, Table 2 and Figs. 21, 22 and 23.

Table 2.

t	x_m	x_i	δ
3	0.599	1.002	0.794
4	0.656	1.107	0.840
5	0.761	1.286	0.938

The diffusion coefficient was recalculated for 25 °C using the viscosity ratio, giving the following result.

Inflexion point method:

$$D_{25°} = 1.29 \; cm^2/day$$

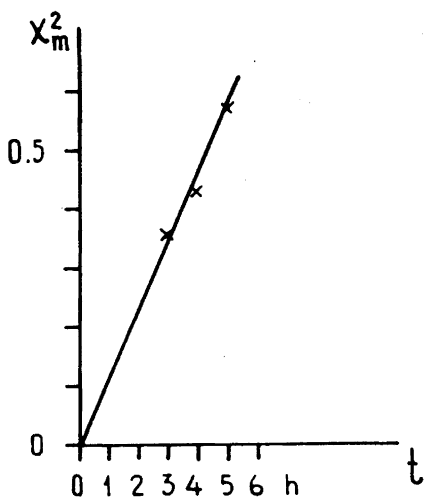"Width" method:

$$D_{25°} = 1.30 \; cm^2/day$$

Fig. 21. Maximum point method for the determination of the diffusion coefficient of NaCl. Expt. 2.
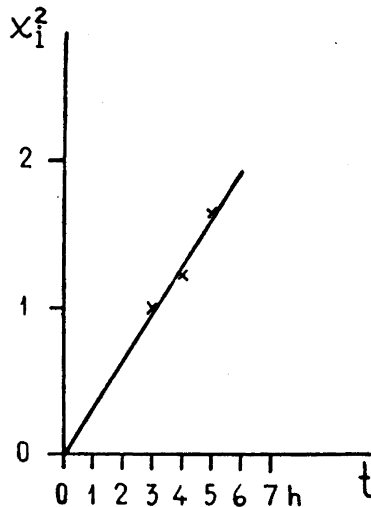

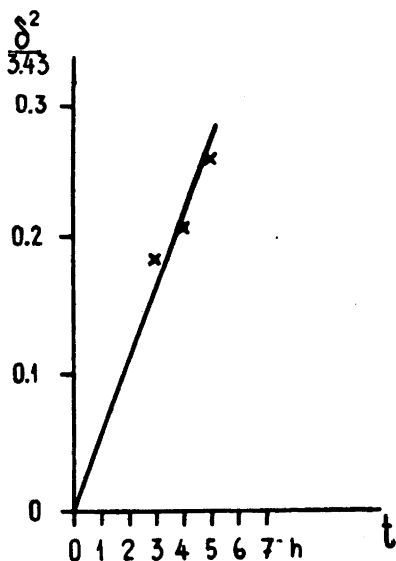
Fig. 22. Inflexion point method. Expt. 2.
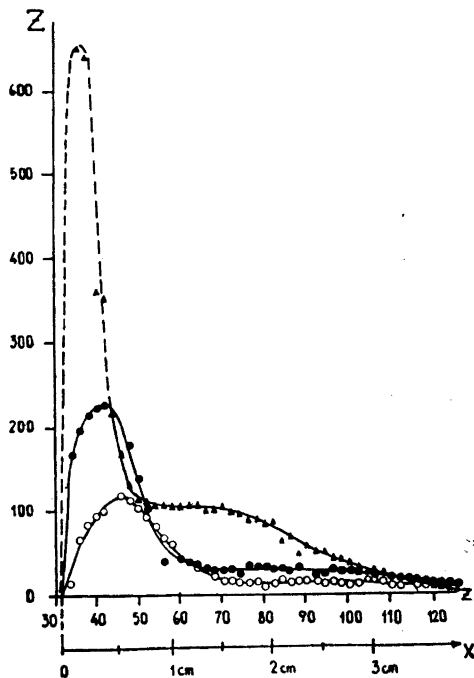

Fig. 23. "Width" method. Expt. 2.

Fig. 24. Expt. 3. 0.6% dextran + 2.4% NaCl at 24.77°. Filled triangles, 12-h curve; filled circles, 35.3-h curve; empty circles, 71-h curve.
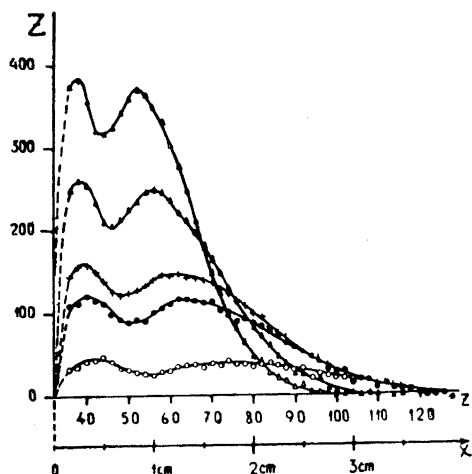
Fig. 25. Expt. 4. 0.1 % dextran + 2.9 % NaCl at 24.77°. Empty triangles, 4-h curve; filled triangles, 6-h curve; crosses, 10-h curve; filled circles, 12-h curve; empty circles, 24.5-h curve.
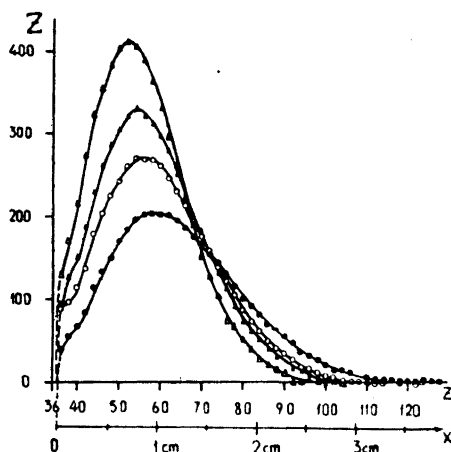

Fig. 26. Expt. 5. 0.03 % dextran + 3 % NaCl at 24.78°. Empty triangles, 4-h curve; filled triangles, 5-h curve; empty circles, 6-h curve; filled circles, 8-h curve.

Maximum point method:

$$D_{25°} = 1.38 \ cm^2/day$$

illustrative of the fact that the maximum point abscissae are less accurately read from the curve diagram than the widths and the influxion point abscissae.

These values can be compared with the following values given by Kortüm and Bockris, *Textbook of Electrochemistry* for the diffusion coefficient of NaCl:

at $c = 0$ $D_{25°}^{-} = 1.39 \ cm^2/day$

$c = 0.5$ $D_{25°} = 1.27 \ cm^2/day$

in fair agreement with the above results. It should, however, be mentioned that the precision determinations of diffusion coefficients approach or attain an accuracy of 0.1 %.

B. Experiments with non-uniform substances

Native dextran as produced by *Leuconostoc mesenterioides* is a polydisperse polysaccharide with molecular weight ranging from 14 000 to 40 000 000. A partially hydrolyzed form with molecular weight of 20 000—200 000 has gained use as a plasma substitute. A commercial preparation, "Macrodex", manufactured by the Pharmacia company, Uppsala, Sweden, contains 6 % partially hydrolyzed dextran and 0.9 % NaCl. The solutions used in the experiments described below were prepared by diluting "Macrodex" and adding the required amount of sodium chloride.

Experiment 3. 0.4 ml of a solution containing 0.6 % dextran and 2.4 % NaCl was injected. The diffusion curves obtained are reproduced in Fig. 24. In this case the dextran gives by far the greatest contribution to the refractive index gradient, which illustrates the facts already pointed out in the theoretical section.

Experiment 4. 0.4 ml of a solution of 0.1 % dextran and 2.9 % NaCl was injected. The diffusion curves are reproduced in Fig. 25. If we assume $R_1 = R_2$ we get

$$\beta = A_1 / A_2 = 2.9/0.1 = 29$$

It is remarkable, and in conformity with the foregoing discussion, how much this small amount of dextran contributes to the refractive index gradient. In fact two distinct peaks in the curve are obtained, the relative positions of which agree fairly well with the relation between the diffusion coefficients.

Experiment 5. 0.4 ml of 0.03 % dextran and 3 % NaCl was injected. The diffusion curves are reproduced in Fig. 26. If $R_1 = R_2$ we have $\beta = A_1/A_2 = 100$. A definite deviation from the curve for pure sodium chloride is seen to occur for low values of x. However, this probably represents the limiting case unless high-molecular impurities can be wholly avoided. In fact, the quantity of dextran injected in this case is only $0.4 \times 0.03 \times 10^{-2}$ g $= 0.12$ mg.

REFERENCES

1. Lamm, O. *Diss.* Uppsala 1937, p. 38.
2. Lamm, O. *Diss.* Uppsala 1937, p. 35.
3. Fürth, R. *Hdb. der phys. u. tech. Mechanik,* vol. VII.
4. Lamm, O. *Diss.* Uppsala 1937, p. 64.
5. Svensson, H. *Nature* **161** (1948) 234.
6. Lamm, O. *Acta Chem. Scand.* **9** (1955) 546.
7. Lamm, O. *Diss.* Uppsala 1937, p. 71.

Received December 3, 1956.